Published in final edited form as:

Cancer Res. 2021 April 15; 81(8): 2044–2055. doi:10.1158/0008-5472.CAN-20-2041.

The miR-181a-SFRP4 axis regulates Wnt activation to drive stemness and platinum resistance in ovarian cancer

Anil Belur Nagaraj[1,#], **Matthew Knarr**[2,#], **Sreeja Sekhar**[9,10], **R. Shae Connor**[4], **Peronne Joseph**[3], **Olga Kovalenko**[3], **Alexis Fleming**[3], **Arshia Surti**[3], **Elmar Nurmemmedov**[5], **Luca Beltrame**[6], **Sergio Marchini**[6], **Michael Kahn**[7], **Analisa DiFeo**[8,9,10,*]

[1]Laboratory Medicine and Pathology, Mayo Clinic, Rochester MN 55902

[2]Department of Obstetrics & Gynecology, Perelman School of Medicine University of Pennsylvania, Philadelphia, PA 19104

[3]Case Comprehensive Cancer Center, Case Western Reserve University, Cleveland, OH 44106

[4]University of Tennessee, Erlanger Health System, Chattanooga, TN

[5]John Wayne Cancer Institute at Providence St. John's Health, Santa Monica, CA 90404

[6]Dept. of Oncology Istituto di Ricerche Farmacologiche "Mario Negri" Milano Italy

[7]Department of Molecular Medicine, Beckman Research Institute of City of Hope, City of Hope Comprehensive Cancer Center, Duarte, CA 91010

[8]Department of Obstetrics & Gynecology, The University of Michigan, Ann Arbor, MI 48109

[9]Department of Pathology, The University of Michigan, Ann Arbor, 48109

[10]The Rogel Cancer Center, The University of Michigan, Ann Arbor, MI 48109

Abstract

Wnt signaling is a major driver of stemness and chemo-resistance in ovarian cancer, yet the genetic drivers that stimulate its expression remain largely unknown. Unlike other cancers, mutations in the Wnt pathway are not reported in high-grade serous ovarian cancer (HGSOC). Hence, a key challenge that must be addressed in order to develop effective targeted therapies is to identify non-mutational drivers of Wnt activation. Using a miRNA sensor-based approach, we have identified miR-181a as a novel driver of Wnt/β-catenin signaling. miR-181a^{high} primary HGSOC cells exhibited increased Wnt/β-catenin signaling, which was associated with increased stem-cell frequency and platinum resistance. Consistent with these findings, inhibition of β-catenin decreased stem-like properties in miR-181a^{high} cell populations and downregulated miR-181a. The Wnt inhibitor SFRP4 was identified as a novel target of miR-181a. Overall, our results demonstrate that miR-181a is a non-mutational activator of Wnt signaling which drives

[*]**Corresponding Author** **Analisa DiFeo, Ph.D.,** Associate Professor, Department of Pathology, Associate Professor, Department of Obstetrics & Gynecology, University of Michigan, Michigan Medicine, Rogel Cancer Center, 1600 Huron Parkway Ann Arbor, MI 48109-5932 Office Number: (734)936-5685, adifeo@med.umich.edu.

[#]Contributed equally

Conflict of Interest: MK has equity in 3+2 Pharma LLC and is a consultant for Fuji Film Pharma and Lynk Pharmaceuticals.

stemness and chemoresistance in HGSOC, suggesting that the miR-181a-SFRP4 axis can be evaluated as a novel biomarker for β-catenin-targeted therapy in this disease.

Introduction

Epithelial ovarian cancer (EOC) is currently the most lethal gynecologic malignancy with an estimated 22,530 new cases and 13,980 deaths in 2020. Thus, novel therapeutic interventions are needed to improve the survival of women affected by this disease[1]. Tumor heterogeneity presents a major barrier towards gaining a better understanding of the molecular underpinnings driving tumor progression, chemo-resistance and tumor-recurrence, thus the development of novel effective therapies to treat EOC is lacking[2,3]. Heterogeneity is a defining feature of EOC, given that the disease can arise from several distinct anatomic locations. The most common site of origin is the fallopian tube surface epithelium which in turn gives rise to the most common EOC subtype, high-grade serous ovarian tumors (HGSOC)[4–8]. HGSOC is characterized by a high degree of genomic instability rather than a small subset of driver mutations which greatly increases the heterogeneity of cancer cells within the tumor. This high degree of tumor heterogeneity ultimately translates to a much higher probability of developing chemo-resistance and recurrence.

Understanding mechanisms driving EOC pathogenesis in the context of heterogeneity forms a crucial component of determining the different signaling pathways that regulate diverse sub-populations of tumor cells in primary ovarian tumors. Current experimental approaches have limited utility to explore this possibility. Classic overexpression or knockdown genetic approaches fail to account for tumor heterogeneity and do not enable analysis of tumor sub-populations. Hence, novel experimental methodologies that can enable isolation and analysis of tumor sub-populations can decipher mechanisms underlying EOC pathogenesis in the context of heterogeneity, thus contributing to the design of successful targeted therapies.

We have developed a miRNA 3'UTR sensor based functional platform[9] to isolate and analyze tumor sub-populations based on miRNA activity[10]. Given that a single miRNA can bind to hundreds of 3'UTRs thus regulating multiple pathways simultaneously, miRNAs constitute efficient targets to dissect tumor heterogeneity since they regulate multiple pathways and can be employed to isolate and analyze multiple tumor-subpopulations as compared to single pathway reporter based approaches. Utilizing this miRNA sensor platform, we found that a miR-181a^{high} subpopulation of cells sorted from primary ovarian tumor cells exhibited stem-like properties *in-vivo*, were enriched in response to continuous cisplatin treatment, and showed activation of major stem cell regulatory pathways[10]. In the current study, we have identified Wnt/β-catenin signaling to be enriched in miR-181a^{high} primary ovarian tumor cells and show that miR-181a driven Wnt signaling promotes stem-like properties. Furthermore, we show that miR-181a activates Wnt signaling by targeting the secreted WNT inhibitor SFRP4. Our study highlights the importance of employing endogenous miRNA activity based experimental approaches to study tumor sub-populations in cancers that can: 1) uncover endogenous regulators of relevant signaling pathways and, 2) enhance the clinical translation of targeted therapies to overcome heterogeneity driven chemo-resistance and tumor-recurrence.

Materials & Methods

Cell Culture & Reagents

Cells were cultured in 10mm plates in a humidified atmosphere (5% CO_2) at 37°C. At 70–90% confluence, trypsin (0.25%)/EDTA solution was used to split the cells which were used until passage 20. Cell culture medium (Corning) was supplemented with 10% FBS (Gibco) and 1% Penicillin-Streptomycin (PS) (Gibco) [OV81.2-CP10 cells (DMEM), HEYA8 cells (RPMI)]. Primary HGSOC cells (OCI-P5X, OV236) were cultured in OCMI-L medium (Liver tumor culture core, University of Miami). OV81.2-CP10 and OV236 are primary HGSOC generated in the DiFeo Laboratory as previously described[10,11]. OCI-P5X cells were purchased from Liver Tumor Culture Core, University of Miami. HEYA8 was obtained from Dr. Anirban Mitra from University of Indiana. All cell lines were maintained below 25–30 passages for all experiments and tested monthly for mycoplasma infection. In addition, the cell lines have been authenticated using genetic profiling via polymorphic short tandem repeat. The following reagents were used in the study: Cisplatin (Mount Sinai Hospital Pharmacy), Lithium chloride (Sigma), iCG-001 (Selleckchem), Sh-β-catenin and Sh-Control vectors (addgene)[11], Top-eGFP plasmid (Addgene), *miR-181a* overexpression and control vector (Biosettia), *miR-181a* antagomiR and control vector (Genecopoeia). Hes1 plasmid was a kind gift from Dr. Barbara Bedogni. Top-FLASH plasmid was a kind gift from Dr. William Scheimann.

Cell Viability Assay

Cells were plated in 12-well plate at 50,000 cells/well and treated the next day with the drugs. After 48hr, cells were then incubated with 3-(4,5-Dimethylthiazolyl) for 2hr and absorbance was measured at 600nm.

Flow Cytometry

BD LSR II was used for flow cytometry analysis with miR-181a sensor and BD FACS Aria was used for miR-181a sensor based sorting.

Immunoblotting

Total protein lysates were prepared from cell pellets using RIPA buffer supplemented with PhosSTOP phosphatase inhibitor and cOmplete protease inhibitor cocktail (Roche). Protein concentration of cell lysates was determined using BCA assay. Western blots were run as described previously[12,13]. Primary and secondary antibodies used are listed below. List of antibodies used in western blots are presented in Supplemental Table 1.

Immunocytochemistry

Immunocytochemistry of cells was performed as previously described[14] wherein cells were seeded in 4 well chamber slides at a density of 70,000 cells per well (approx. 70% confluent) and were allowed to grow for 48 hr. The cells were washed with 1X PBS and then fixed with 4% paraformaldehyde for 10 min. Cells were washed with 1X PBS three times for 5 min each followed by permeabilization with 0.01% (v/v) Triton X100 (Sigma) for 10 minutes. The cells were washed 3X with 1X PBS for 5 min each followed by blocking in 3%

bovine serum albumin for 1 hr. The cells were then incubated with anti-active β-catenin primary antibody (1:500 dilution) overnight. The cells were then washed 3X with PBS for 5 min each followed by incubation with anti-rabbit Dylight488 conjugated secondary antibody (Thermo Fisher cat. #35553 1:100 dilution) in 3% BSA for 1 hr. After incubation with the secondary antibody the cells were then washed 3X with PBS for 5 min each followed by counterstaining with ActinRed 555 ReadyProbes reagent (Invitrogen) for 30 min. After counterstaining the cells were then washed 3X with PBS for 5 min each followed by mounting with Prolong Diamond mountant w/DAPI. Cells were imaged using a Leica DMI6000 inverted microscope. LAS-X imaging software was used to analyze images for fluorescence intensity. Cells were imaged in biological triplicate with each biological replicate consisting of a minimum of 30 cells analyzed.

In Vivo Tumor Formation Assays

All in vivo experiments were conducted according to protocols approved by the Animal Research Committee at University of Michigan.

Subcutaneous Tumor Formation: For the HEYA8 miR-181a sensor study, 2×10^4 cells were injected subcutaneously in a 1:1 mixture of DMEM media and Matrigel matrix (Corning). For each group (HEYA8 miR-181a^{Low}, HEYA8 miR-181a^{High}) a total of 10 mice were used per group with one injection site per mouse for a total of 10 tumor injections per group. Tumors were measured every other day for up to 40 days. The tumor formation endpoint was predetermined as the time point where at least one group had a majority (>5/10 mice) of mice with palpable tumors. At 40 days all mice were euthanized, and tumors were recovered for endpoint measurements, RNA, protein, and histological analysis. For the HEYA8 ICG study, 2.5×10^5 cells were injected subcutaneously in a 1:1 mixture of DMEM media and Matrigel matrix (Corning). Post-injection mice were randomized into 4 treatment groups; Vehicle, Cisplatin, ICG-001, and Cisplatin + ICG-001 with at least 6 mice per group. Mice were enrolled in the study and treatment was begun when measured tumor volume was ≥100 mm^3. Vehicle mice were injected with PBS solution twice a day. Cisplatin mice were injected IP with 2 mg/kg Cisplatin every other day. ICG-001 mice were injected IP with 100 mg/kg ICG-001 twice per day. Cisplatin + ICG-001 mice were injected IP with 2 mg/kg Cisplatin every other day and were injected IP with 100 mg/kg ICG-001 twice per day. Mice were treated for 19 days with the primary endpoint reached when all of the mice enrolled in the vehicle control group reached a tumor volume of ≥1600 mm^3. Mice with tumors ≥2500 mm^3 prior to the primary endpoint were euthanized for animal welfare reasons. Once the primary endpoint was reached, all mice were euthanized, and tumors were recovered for endpoint measurements, RNA, protein, and histological analysis.

Lentiviral Transduction

For lentiviral transfection, Lenti Starter Kit (System Biosciences, CA) was used. Briefly, 293T cells (ATCC) were transduced with 2μg plasmid and 10μg of pPACKH1-plasmid mix with Lipofectamine 2000 (Life Technologies, CA). 48hr later, virus particles were harvested and precipitated. Target cells were transduced by plating 100,000 cells/well in a 6 well plate with virus particles and 4μg/mL polybrene (Santa Cruz Biotechnologies, CA)

Limiting Dilution Tumor Sphere Formation Assay

For limiting dilution sphere assays, BD FACS Aria II sorter was used to sort cells directly into 96-well ultra-low attachment plates (Corning, NY) in 200μl mammocult media (STEMCELL Technologies, Vancouver, Canada) per well. After 14 days, the number of wells with tumor spheres was counted and the data was analyzed by Extreme Limited Dilution Analysis [ELDA] platform to determine the stem cell frequency.

Luciferase Reporter Assay

Top-Flash plasmid (1μg) or HES1 plasmid (1μg) and renilla (150ng) were co-transfected using lipofectamine 2000 (Life Technologies). SFRP4 3'UTR reporter plasmid (1μg) was transfected using Lipofectamine 2000. Luciferase activities were analyzed using the Dual-Luciferase Reporter Assay System (Promega) with data normalization to the corresponding renilla values.

RNA Extraction & Quantitative Real-Time PCR

Total RNA was extracted using the Total RNA Purification Plus Kit (Norgen Biotek, ON, Canada). For mRNA analysis, cDNA synthesis from 1μg of total RNA was done using the Transcriptor Universal cDNA Master kit (Roche, IN, USA). SYBR green-based Real-time PCR was subsequently performed in triplicate using SYBR green master mix (Roche) on the Light Cycler 480 II real time PCR machine (Roche). For miRNA expression assays, cDNA synthesis was done using Taqman gene expression assays (Life Technologies, Carlsbad, CA) and subsequent Real-time PCR was performed using Taqman universal PCR mastermix, no AmpErase UNG buffer (Life Technologies, Carlsbad, CA) with corresponding probes and primer mix (Taqman gene expression assays).

Generation of OVCAR4 cisplatin-resistant cells.

Cisplatin-sensitive parental OVCAR4 cells were cultured in RPMI medium supplemented with 2% serum. To generate, cisplatin-resistant OVCAR4-CP cells, parental cells were initially treated with 10μM cisplatin, and then dose was gradually increased to 500μM in the course of 14 days.

Culturing and treatment of OVCAR4 cells

Cisplatin-sensitive parental OVCAR4 cells were cultured in RPMI medium supplemented with 2% serum. To generate, cisplatin-resistant OVCAR4-CP cells, parental cells were initially treated with 10μM cisplatin, and then dose was gradually increased to 500μM in the course of 14 days. In order to compare cisplatin-sensitivity of OVCAR4-CP and parental cells, cell viability assay was performed (Supplemental Figure 7) in 96-well format. 1000 cells were dispensed in 100μl RPMI medium supplemented with 2% serum. Cells were treated with varying doses of cisplatin (10–600μM), incubated for 72 hours, after which viability was measured using Alamar blue method.

Subsequently, cells were tested for WNT modulators LGK-974 and ICG-001 in dose-response manner (20 – 40.000nM) as described above. Hence, IC50 for these drugs was calculated (Supplemental Figure 7). Later, parental and cisplatin-resistant cells were treated

DMSO, LGK-974 (3μM) and ICG-001 (3μM) for 72 hours, then harvested for RNA extraction.

Statistical Analysis

Unless otherwise noted, data are presented as mean ± SD from three-independent experiments, and Student's *t*-test (two-tailed) was used to compare two groups ($P<0.05$ was considered significant) for independent samples.

Results

miR-181a ^{high} EOC stem-like tumor populations exhibit increased cisplatin resistance and β-catenin protein expression

Wnt/β-catenin signaling has consistently been shown to be a critical driver of EOC recurrence and cisplatin resistance[11,12,15–18]. Unlike other cancers, Wnt/β-catenin signaling components are not known to exhibit mutations in EOC, particularly in high-grade serous ovarian cancer. In addition, upstream regulators of this pathway are not well understood in the context of HGSOC[19,20]. Hence, we set out to explore the utility of our miRNA sensor platform to study the potential regulation of Wnt/β-catenin signaling by miR-181a. miR-181a is reported to induce Wnt/β-catenin signaling in Acute Lymphoblastic Leukemia (ALL)[21] but the regulation of Wnt/β-catenin signaling by miR-181a has not explored in EOC.

In order to assess potential functional interaction between miR-181a and Wnt/β-catenin signaling in EOC, we first assessed miR-181a 3'UTR activity in multiple EOC cell lines including HEYA8 cells and two primary cell lines developed from primary high-grade serous ovarian cancer OCI-P5X cells and cisplatin resistant OV81.2-CP10 cells [11,22]. Using our miR-181a sensor, we dichotomized each cell line into miR-181a^{High} and miR-181a^{Low} subpopulations (Supplemental Figure 1) and confirmed that the miR-181a^{High} subpopulations exhibited increased stem cell capacity using an *invitro* extreme limiting dilution sphere formation assay (ELDA) (Figure 1A). The HGSOC sensor miR-181a^{High} cells exhibited a 3–6 fold increase in miR-181a expression vs miR-181a^{Low} cells (Figure 1B) and western blot analysis showed that miR-181a^{High} cells exhibited increased β-catenin protein expression (Figure 1C). We also observed that the miR-181a^{High} HGSOC cells exhibited higher IC50 values in response to cisplatin treatment as compared to the miR-181a^{low} cells (approx. increase of 2–3 fold in IC50 between miR-181a^{High} vs miR-181a^{Low} HGSOC cells) (Figure 1D &1E). Furthermore, miR-181a functional knockdown in OVCAR3 cells using stable miR-181a decoy vectors[23] confirmed that targeted inhibition of miR-181a results in decreased survival, increased sensitivity to cisplatin and reduced tumor-sphere formation ability (Supplemental Figure 2A–E).

Wnt/β-catenin signaling is enriched in miR-181a^{high} cells in EOC

To determine if miR-181a is a novel regulator of Wnt/β-catenin signaling in EOC, we next assessed the status of this pathway in miR-181a^{high} and miR-181a^{low} sub-populations. Examination of downstream Wnt transcriptional targets showed increase in stemness markers such as ALDH, CD133, and SOX2, as well as canonical Wnt targets such as

CTNNB1, TCF7, LGR5, and LEF1 in the miR-181a^{high} HGSOC (Figure 2A). Using immunofluorescence, we examined the levels of active β-catenin. We observed a 3–5 fold increase in active β-catenin levels in the HGSOC miR-181a^{high} sub-populations (Figure 2B–C). Next, we evaluated nuclear β-catenin activity using TOP-eGFP and TOPFLASH reporter assays. A 2–6 fold increase in WNT signaling transcriptional activation was observed in the miR-181a^{high} HGSOC (Figure 2D). We further assessed the effects of miR-181a upregulation on Wnt signaling by overexpressing miR-181a in a high-grade serous PDX derived cell line (OV81.2)[11](Supplemental Figure 3A–B). We found that miR-181a overexpression increased sphere formation by 4-fold, lead to cisplatin resistance and significantly enhanced the expression of both total and active β-catenin further confirming that miR-181a activates Wnt signaling. Collectively, these results reveal that miR-181a activity is significantly associated with increased Wnt/β-catenin signaling in EOC cells, and suggest that the miR-181a/β-catenin axis is functionally important in the regulation of stem-like properties.

Wnt/β-catenin inhibitor SFRP4 is a novel target of miR-181a

We next looked at the relative expression of several Wnt inhibitors that are predicted to be targets of miR-181a (*SFRP4,BTRC,APC, and NLK1*) in order to ascertain what could be driving the upregulation of Wnt/β-catenin signaling in miR-181a^{high} EOC. Interestingly, SFRP4 was the only candidate gene whose mRNA and protein expression was consistently low in the miR-181a^{high} EOC cells suggesting that it could be a potential target of miR-181a (Figure 3A&B). Since SFPR4 is reported to inhibit Wnt/β-catenin signaling in EOC[20], downregulation of SFRP4 could be one of the mechanisms by which miR-181a activates Wnt/β-catenin signaling. In order to confirm direct binding of miR-181a on the 3'UTR of SFRP4, we performed 3'UTR luciferase assays and found that the SFRP4 3'UTR expression in the miR-181a^{high} cells was significantly decreased (Figure 3C). Consistent with these findings, we also found that miR-181a overexpression decreased SFRP4 3'UTR activity in OV81.2 cell line (Supplemental Figure 3C). Next, we assessed whether miR-181a targeting of SFRP4 affected *in-vivo* tumor formation using the HEYA8 sensor cells. We have previously shown that miR-181a^{High} cells have increased tumorgenicity potential, increased tumor kinetics, and total tumor burden compared to miR-181a^{Low} cells. Therefore, we next wanted to assess whether these tumors had differential expression of β-catenin and SFRP4[10]. We were able to confirm our previous findings, and also found that the miR-181a^{Low} tumors had significantly decreased expression of β-catenin and increased expression of SFRP4 indicating repression of WNT signaling in the tumors by SFRP4 (Figure 3D–H). In order to confirm the clinical relevance of the miR-181a/SFRP4 axis in EOC patient tumors, we next assessed whether we could utilize the miR-181a sensor platform in primary patient tumor cells. We found that in tumor cells isolated from primary recurrent high-grade serous ovarian cancer (OV236) SFRP4 expression was low in the miR-181a^{High} sub-population as compared to miR-181a^{Low} sub-population (Supplemental Figure 4A–B). Furthermore, we found that in a cohort of 23 matched primary and recurrent samples from stage III-IV high-grade serous ovarian cancer patients miR-181a expression was increased (4-fold increase primary vs recurrent) and SFRP4 expression was decreased (−0.5-fold decrease primary vs recurrent) in the primary vs recurrent tumors (Figure 3I). Interestingly, we also found that the recurrent tumors had a significant upregulation of CD44

and β-catenin (Figure 3I). Collectively, these results identify SFRP4 as a potentially clinically relevant target of miR-181a in EOC which leads to the activation of the Wnt/β-catenin signaling pathway.

SFRP4 inhibits tumor initiating cell properties in miR-181a EOC cells

Next, in order to determine whether SFRP4 was driving the stem-like properties observed in the miR-181a^{High} we re-expressed SFRP4 lacking a 3'UTR in these cells and ascertained whether it could reverse these properties. SFRP4 re-expression in the OCI-P5X miR-181a^{High} cells (Figure 4A–B) resulted in significant decrease in active β-catenin expression and a robust decrease in tumor-sphere formation capacity (Stem Cell Frequency Ratio of 1:26 vs 1:3 in OCI-P5X miR-181a^{High} pSFRP4 vs pTOL cells) (Figure 4C–D). Primary HGSOC OCI-P5X miR-181a^{High} pSFRP4 cells also had decreased expression of CSC markers including ALDH1, CD44, and CD133 (Figure 4E). Wnt signaling markers and TOPFLASH luciferase reporter activity was also significantly decreased in the miR-181a^{High} pSFRP4 cells (Figure 4E–F). Taken together, these data show that the increase in TIC properties driven by miR-181a Wnt activation is mediated by miR-181a targeting of SFRP4.

Inhibition of miR-181a activated Wnt signaling decreases EOC tumor initiating cell properties

We next wanted to confirm that miR-181a activation of Wnt/β-catenin signaling was responsible for the increase in stem-like properties observed in the HGSOC miR-181a^{High} cells. ShRNA mediated downregulation of β-catenin in HEYA8 miR-181a^{High} and OV81.2-CP10 miR-181a^{High} cells decreased the expression of β-catenin driven stem cell markers which correlated with decreased stem-cell frequency in these cells, suggesting that β-catenin functions downstream of miR-181a (Figure 5A–C). Next, we employed the use of the ICG-001 compound to specifically inhibit β-catenin/CBP transcriptional activity and assess whether suppression of β-catenin/CBP would selectively kill miR-181^{high}/ Wnt^{high} cells or promote differentiation to a miR-181 low population(Figure 5D). We found that ICG-001 treatment enriched for miR-181^{low} and eliminated the majority of miR-181^{high} cell and significantly decreasing miR-181a expression. (Figure 5E & 5F). In addition, ICG-001 decreased the expression of stem cell markers and downstream Wnt activation markers (Figure 5G). Furthermore, ICG-001 also decreased tumor sphere formation and stem-cell frequency (stem cell frequency ratio of 1:2.26 vs 1:100 in HEYA8 miR-181a^{high} DMSO vs ICG-001 treated cells) further confirming that β-catenin functions downstream of miR-181a (Figure 5H–I).

Next, to further assess whether miR-181a acts upstream or downstream of β-catenin we activated the Wnt signaling pathway using LiCl in both the miR-181a^{high} and miR-181a^{low} cells, interestingly we found that only in the miR-181a^{low} cells did Wnt activation lead to a significant increase in tumor spheres (Supplemental Figure 5A–E), indicating that Wnt activation in these cells was still able to induce stem-like properties. Conversely, in the miR-181a^{high} cells there was no increase in tumor spheres, however, the sphere size did significantly increase suggesting that LiCl induced Wnt activation in miR-181a^{high} cells was most likely still able to induce proliferative genes but not stem cell signatures.

Lastly, to expand on these findings we treated the OV81.2 miR-181a overexpressing cells with ICG-001 and found that it was able to decrease tumor sphere formation in these cisplatin resistant tumor spheres confirming that miR-181a induced platinum-resistance and increased stem-like properties were mediated via the upregulation of Wnt//β-catenin pathway (Supplemental Figure 6). These results suggest that Wnt/CBP/β-catenin inhibitors such as ICG-001/PRI-724 are able to therapeutically target miR-181a/Wnt high EOC cells responsible for tumor progression.

Therapeutic targeting of miR-181a-Wnt signaling decreases EOC tumor growth *in-vivo*

Finally, we assessed the therapeutic efficacy of ICG-001 treatment *in-vivo* using HEYA8 cells (which have endogenously high expression of miR-181a and Wnt activity). We found that mice treated with either ICG-001 or ICG-001/Cisplatin combination showed a significant reduction in tumor volume compared to vehicle treated mice, whereas mice treated only with cisplatin did not show a significant decrease in tumor volume (Figure 6A). Importantly, the tumors treated with ICG-001 or ICG-001/Cisplatin combination showed decreased levels of miR-181a compared to vehicle control tumors, whereas the Cisplatin treated tumors did not and no overt toxicities were noted (Figure 6B), (Supplemental Figure 7A). We have also confirmed that other Wnt inhibitors including LGK-974 can decrease the expression of miR-181a in OVCAR4 cisplatin-resistant models (Supplemental Figure 8A–C). We then profiled the correlation between miR-181a or SFRP4 expression and tumor volumes from this *in-vivo* tumor study and found that miR-181a expression positively correlated with tumor volume (Spearman correlation coefficient: $r = 0.4976$, $P = 0.0083$) while SFRP4 expression negatively correlated with tumor volume (Spearman correlation coefficient: $r = -0.3823$, $P = 0.046$) (Figure 6C–D). We also found that ICG-001 treatment lead to a decrease in several Wnt and stem cell markers (Supplemental Figure 9A). Importantly, matched miR-181a and SFRP4 expression within the same tumor were also inversely correlated (Spearman correlation coefficient: $r = -0.4656$, $P = 0.0114$) (Figure 6E). In addition, the tumors treated with ICG-001 (which targets the miR-181a-Wnt axis) had lower expression levels of miR-181a and higher expression levels of SFRP4 (Figure 6E). This indicated that ICG-001 was able to target the miR-181a-SFRP4 axis and miR-181a may serve as a surrogate biomarker for Wnt targeted therapies.

Discussion

Disease recurrence remains one of the primary barriers in successfully treating ovarian cancer patients. While HGSOCs are initially sensitive to platinum-based therapies and can remain responsive even after multiple rounds of chemotherapy, eventually 80–90% of patients will develop recurrent disease that is cisplatin resistant and no longer responds to chemotherapy. One of the main reasons for the high rate of recurrence is that HGSOC progression is not defined by recurrent driver mutations, but rather by large scale genomic instability involving frequent copy number gains and losses across the entire genome. As such, a high degree of clonal heterogeneity within the tumor is present prior to initial treatment with chemotherapy. The abundance of this intratumor heterogeneity dramatically increases the probability of recurrence due to the increased frequency of resistant sub-clones.

Studying tumor sub-populations in cancers offers an approach to understand heterogeneity, and the miRNA sensor model that we have developed attempts to provide such an approach. The miRNA sensor platform can be successfully employed towards deciphering miRNA-signaling pathway interactions in tumor sub-populations based on endogenous activity of the miRNA of interest. In the present study, we utilized a miR-181a sensor to reveal how this sensor platform can not only identify key miRNAs driving tumor phenotype, but also identify the downstream pathways that can be targeted. We have shown that miR-181a^{high} cell populations are able to promote recurrence and cisplatin resistance through the upregulation of Wnt/β-catenin signaling. Further analysis identified miR-181a as a novel upstream activator of Wnt/β-catenin signaling via the inhibition of SFRP4. Both genetic and chemical inhibition of this signaling pathway using shRNA mediated β-catenin downregulation or ICG-001 in miR-181a^{high} cells decreased stem-like properties, thus identifying β-catenin as a functional component of miR-181a^{high} tumor cells and as a downstream effector of miR-181a in driving stem-like properties in HGSOC. This is further confirmed when we observed that activation of the Wnt signaling pathway in miR-181^{high} cells did not lead to an increase in tumor spheres as it did in miR-181^{low} cells suggesting that miR-181a induced activation of Wnt had already enriched for stem-like cells.

Wnt/β-catenin targeted therapies have been and are still currently being explored in cancer treatment[24], however identifying biomarkers predictive of response to Wnt/β-catenin targeted therapy has still remained a challenge given the complexity of this pathway. Our results show that pharmacologic targeting of β-catenin resulted in robust tumor growth inhibition which was associated with decreased miR-181a and increased SFRP4. Given that circulating miR-181a can be detected in ovarian cancer patient serum[25,26] and SFRP4 is a secreted factor, they may represent potential biomarkers for β-catenin targeted therapies. It has been shown that low SFRP4 expression is reported to correlate with poor prognosis in ovarian cancer[27], which correlates with numerous previous observations that high miR-181a expression is indicative of poor prognosis in ovarian cancer [8,13,14,28,29]. Furthermore, inverse correlation between miR-181a and SFRP4 in primary vs. recurrent ovarian tumors further asserts the clinical importance of miR-181a/SFRP4 axis as a potential biomarker for Wnt targeted therapy in HGSOC. This clinical correlation was further confirmed by miR-181a sensor sorting in primary recurrent ovarian tumor cells. High miR-181a expression correlated with low SFRP4 expression in recurrent ovarian tumor sub-populations differing in miR-181a activity. These results highlight the importance of studying miRNA-pathway interactions in tumor sub-populations to enable identification of novel biomarkers for targeted therapies in cancers. Interestingly, downregulation of miR-181a by pharmacologic inhibition of β-catenin suggests a potential upstream regulation of miR-181a by β-catenin itself. Further experiments are necessary to understand if there is a double positive feedback loop between miR-181a and Wnt/β-catenin signaling in HGSOC.

To summarize, using a novel experimental approach that enables studying tumor sub-populations based on miRNA activity in the context of heterogeneity, we have identified miR-181a as a novel driver of Wnt activity in HGSOC. Our results suggest that miR-181a-SFRP4 axis can be evaluated as a potential biomarker to predict response to β-catenin targeted therapy in HGSOC.

Supplementary Material

Refer to Web version on PubMed Central for supplementary material.

Acknowledgements:

The authors would like to thank several core facilities within the Case Comprehensive Cancer Center (P30CA043703) including the Athymic Animal and Preclinical Therapeutics Core. The authors would like to thank the Rogel Cancer Center at the University of Michigan (P30CA046592) for pilot funds, in support of this project. This work was supported by grants from The National Cancer Institute, R01CA197780 (A.D.), Department of Defense, OC150553 (A.D.), The Young Scientist Foundation (A.D.), and CWRU Pharmacology Department MTTP Training Grant (T32GM008803-11A1). In addition, we would like to thank all the generous donors and Foundations who have supported the DiFeo lab and strive to improve the outcomes of ovarian cancer patients including Norma C. and Albert I. Geller, The Silver Family Foundation and Jacqueline E Bayley (JEB) Foundation.

References

1. Siegel RL, Miller KD, Jemal A. Cancer statistics, 2020. CA Cancer J Clin 2020; 70: 7–30. [PubMed: 31912902]
2. Choi YP, Shim HS, Gao M-Q, Kang S, Cho NH. Molecular portraits of intratumoral heterogeneity in human ovarian cancer. Cancer Lett 2011; 307: 62–71. [PubMed: 21481528]
3. Dagogo-Jack I, Shaw AT. Tumour heterogeneity and resistance to cancer therapies. Nat. Rev. Clin. Oncol. 2018; 15: 81–94. [PubMed: 29115304]
4. Perets R, Wyant GA, Muto KW, Bijron JG, Poole BB, Chin KT et al. Transformation of the Fallopian Tube Secretory Epithelium Leads to High-Grade Serous Ovarian Cancer in Brca;Tp53;Pten Models. Cancer Cell 2013; 24: 751–765. [PubMed: 24332043]
5. Karst AM, Levanon K, Drapkin R. Modeling high-grade serous ovarian carcinogenesis from the fallopian tube. Proc Natl Acad Sci 2011; 108: 7547–7552. [PubMed: 21502498]
6. Vermeulen L, De Sousa E Melo F, van der Heijden M, Cameron K, de Jong JH, Borovski T et al. Wnt activity defines colon cancer stem cells and is regulated by the microenvironment. Nat Cell Biol 2010; 12: 468–476. [PubMed: 20418870]
7. Hassan KA, Wang L, Korkaya H, Chen G, Maillard I, Beer DG et al. Notch pathway activity identifies cells with cancer stem cell-like properties and correlates with worse survival in lung adenocarcinoma. Clin Cancer Res 2013; 19: 1972–1980. [PubMed: 23444212]
8. Nagaraj AB, Joseph P, DiFeo A. miRNAs as prognostic and therapeutic tools in epithelial ovarian cancer. Biomark Med 2015; 9: 241–257. [PubMed: 25731210]
9. Mullokandov G, Baccarini A, Ruzo A, Jayaprakash AD, Tung N, Israelow B et al. High-throughput assessment of microRNA activity and function using microRNA sensor and decoy libraries. Nat Methods 2012; 9: 840–846. [PubMed: 22751203]
10. Belur Nagaraj A, Joseph P, Ponting E, Fedorov Y, Singh S, Cole A et al. A miRNA-Mediated Approach to Dissect the Complexity of Tumor-Initiating Cell Function and Identify miRNA-Targeting Drugs. Stem Cell Reports 2019; 12: 122–134. [PubMed: 30629937]
11. Nagaraj AB, Joseph P, Kovalenko O, Singh S, Armstrong A, Redline R et al. Critical role of Wnt/β-catenin signaling in driving epithelial ovarian cancer platinum resistance. Oncotarget 2015; 6: 23720–34. [PubMed: 26125441]
12. Condello S, Morgan CA, Nagdas S, Cao L, Turek J, Hurley TD et al. β-Catenin-regulated ALDH1A1 is a target in ovarian cancer spheroids. Oncogene 2015; 34: 2297–2308. [PubMed: 24954508]
13. Parikh A, Lee C, Peronne J, Marchini S, Baccarini A, Kolev V et al. microRNA-181a has a critical role in ovarian cancer progression through the regulation of the epithelial-mesenchymal transition. Nat Commun 2014; 5: 2977. [PubMed: 24394555]
14. Knarr M, Nagaraj AB, Kwiatkowski LJ, DiFeo A. miR-181a modulates circadian rhythm in immortalized bone marrow and adipose derived stromal cells and promotes differentiation through the regulation of PER3. Sci Rep 2019; 9. doi:10.1038/s41598-018-36425-w.

15. Cojoc M, Peitzsch C, Kurth I, Trautmann F, Kunz-Schughart LA, Telegeev GD et al. Aldehyde dehydrogenase is regulated by β-Catenin/TCF and promotes radioresistance in prostate cancer progenitor cells. Cancer Res 2015; 75: 1482–1494. [PubMed: 25670168]
16. Sarabia-Sánchez MÁ, Alvarado-Ortiz E, Toledo-Guzman ME, García-Carrancá A, Ortiz-Sánchez E. ALDHHIGH Population Is Regulated by the AKT/β-Catenin Pathway in a Cervical Cancer Model. Front Oncol 2020; 10: 1039. [PubMed: 32766133]
17. Jiang R, Niu X, Huang Y, Wang X. β-Catenin is important for cancer stem cell generation and tumorigenic activity in nasopharyngeal carcinoma. Acta Biochim Biophys Sin (Shanghai) 2015; 48: 229–237.
18. Pandit H, Li Y, Li X, Zhang W, Li S, Martin RCG. Enrichment of cancer stem cells via β-catenin contributing to the tumorigenesis of hepatocellular carcinoma. BMC Cancer 2018; 18: 783. [PubMed: 30075764]
19. Arend RC, Londoño-Joshi AI, Straughn JM, Buchsbaum DJ. The Wnt/β-catenin pathway in ovarian cancer: A review. Gynecol Oncol 2013; 131: 772–779. [PubMed: 24125749]
20. Ford CE, Jary E, Ma SSQ, Nixdorf S, Heinzelmann-Schwarz V a., Ward RL. The Wnt Gatekeeper SFRP4 Modulates EMT, Cell Migration and Downstream Wnt Signalling in Serous Ovarian Cancer Cells. PLoS One 2013; 8: 1–7.
21. Lyu X, Li J, Yun X, Huang R, Deng X, Wang Y et al. MiR-181a-5p, an inducer of Wnt-signaling, facilitates cell proliferation in acute lymphoblastic leukemia. Oncol Rep 2017; 37: 1469–1476. [PubMed: 28184923]
22. Ince TA, Sousa AD, Jones MA, Harrell JC, Agoston ES, Krohn M et al. Characterization of twenty-five ovarian tumour cell lines that phenocopy primary tumours. Nat Commun 2015; 6: 7419. [PubMed: 26080861]
23. Brown BD, Naldini L. Exploiting and antagonizing microRNA regulation for therapeutic and experimental applications. Nat. Rev. Genet 2009; 10: 578–585. [PubMed: 19609263]
24. Krishnamurthy N, Kurzrock R. Targeting the Wnt/beta-catenin pathway in cancer: Update on effectors and inhibitors. Cancer Treat. Rev. 2018; 62: 50–60. [PubMed: 29169144]
25. McIntosh MW, Drescher C, Karlan B, Scholler N, Urban N, Hellstrom KE et al. Combining CA 125 and SMR serum markers for diagnosis and early detection of ovarian carcinoma. Gynecol Oncol 2004; 95: 9–15. [PubMed: 15385104]
26. Elias KM, Fendler W, Stawiski K, Fiascone SJ, Vitonis AF, Berkowitz RS et al. Diagnostic potential for a serum miRNA neural network for detection of ovarian cancer. 2017; : 1–28.
27. Jacob F, Ukegjini K, Nixdorf S, Ford CE, Olivier J, Caduff R et al. Loss of secreted frizzled-related protein 4 correlates with an aggressive phenotype and predicts poor outcome in ovarian cancer patients. PLoS One 2012; 7. doi:10.1371/journal.pone.0031885.
28. Calura E, Paracchini L, Fruscio R, Di Feo A, Ravaggi A, Peronne J et al. A prognostic regulatory pathway in stage I Epithelial Ovarian Cancer: new hints for the poor prognosis assessment. Ann Oncol 2016; : mdw210.
29. Knarr M, Kwiatkowski LJ, McAnulty J, Skala S, Arvil S, et al. A miR-181a initiates and perpetuates oncogenic transformation through the regulation of innate immune signaling. Nat Commun. 2020; 11; 3231 [PubMed: 32591511]

Statement of significance:

These results demonstrate that miR-181a is an activator of Wnt signaling which drives stemness and chemoresistance in HGSOC and may be targeted therapeutically in recurrent disease.

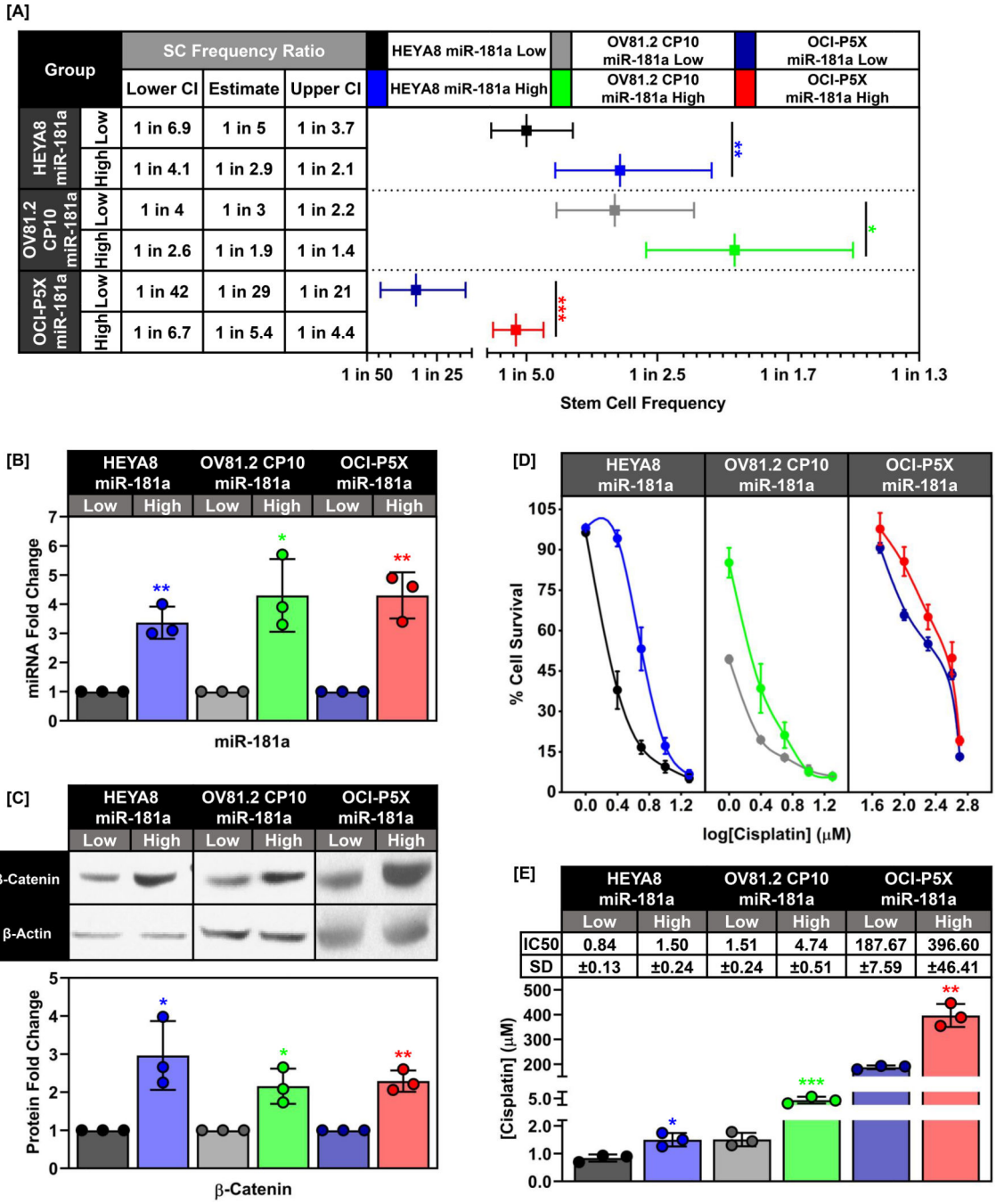

Figure 1: miR-181a^{High} EOC Tumor Initiating Cells exhibit increased cisplatin resistance and β-catenin protein expression

(A) Graph of log(Fraction Non-Responding) vs number of cells (left) and Stem Cell Frequency Ratio for HEYA8 miR-181a^{Low} and miR-181a^{High} cells, OV81.2 CP10 miR-181a^{Low} and miR-181a^{High} cells, and OCI-P5X miR-181a^{Low} and miR-181a^{High} cells. (B) Graph of miR-181a expression in miR-181a^{Low} vs miR-181a^{High} EOC cell lines. (C) Western blots showing β-catenin expression in miR-181a^{Low} vs miR-181a^{High} EOC cell lines with quantification below. (D) Graph showing cell viability dose-response curves for miR-181a^{Low} vs miR-181a^{High} EOC cell lines in response to cisplatin treatment. (E) Graph

showing calculated IC50 values for miR-181a^{Low} vs miR-181a^{High} EOC cell lines in response to cisplatin treatment. All data are representative of 3 independent experiments. * = $p<0.05$, ** = $p<0.005$, *** = $p<0.0005$. Error bars indicate ±standard deviation unless otherwise stated. Error bars for the stem cell frequency graphs indicate upper and lower 95% confidence intervals. Abbreviations: NR- Non-Responding, SC- Stem Cell.

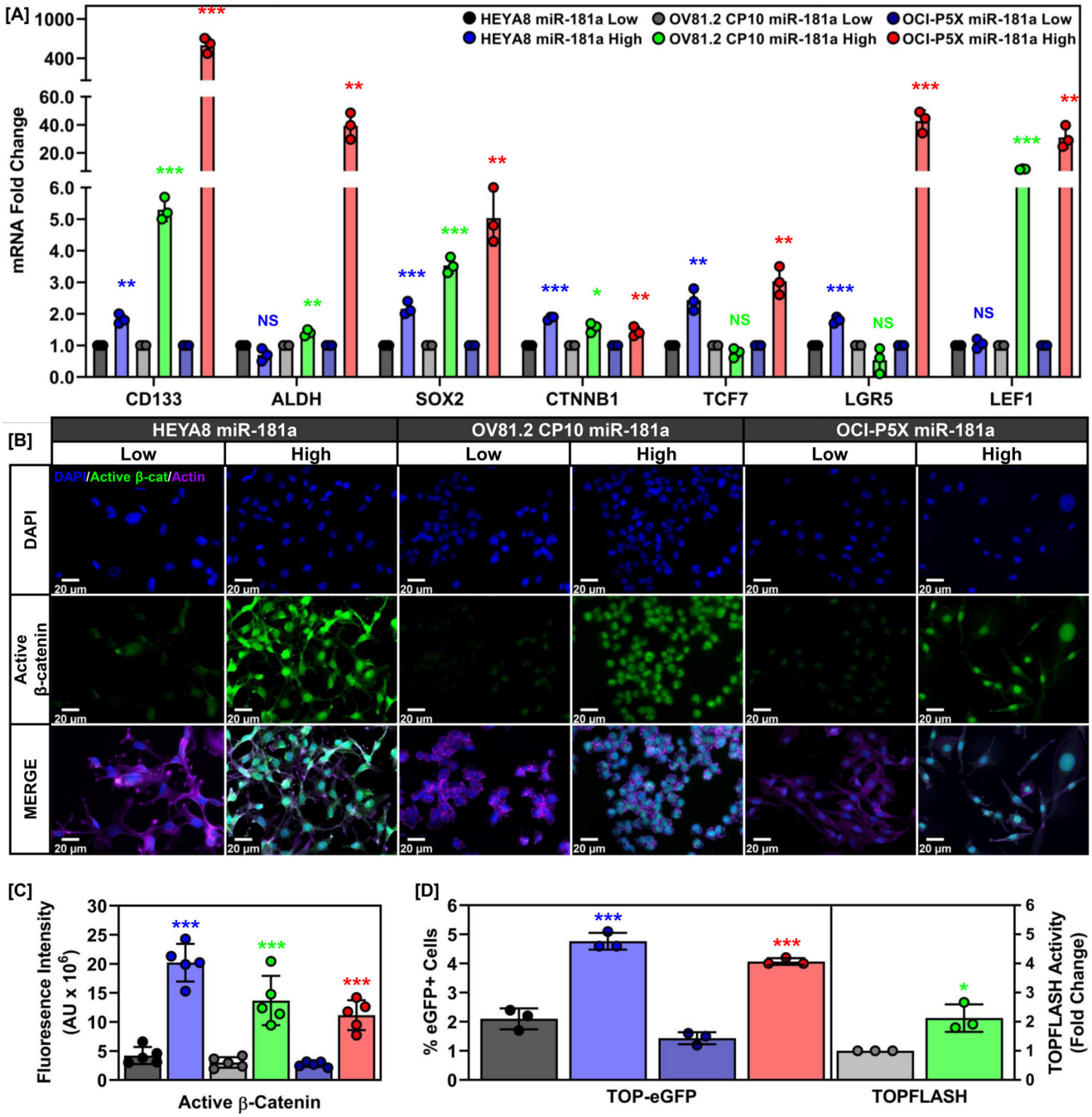

Figure 2: Wnt/β-catenin signaling is enriched in miR-181a high cells in EOC

(A) Graphs of stemness and WNT marker expression in the miR-181a^{Low} vs miR-181a^{High} EOC cells. (B) Representative immunofluorescence micrographs of miR-181a^{Low} and miR-181a^{High} EOC cells stained for active β-catenin. (C) Quantification of immunofluorescence micrographs for active β-catenin. (D) Graph of TOP-eGFP reporter activity for HEYA8, OCI-P5X, and OV81.2 CP10 miR-181a^{Low} vs miR-181a^{High} EOC cells. All data are representative of 3 independent experiments. * = p<0.05, ** = p<0.005,

*** = p<0.0005. Error bars indicate ±standard deviation unless otherwise stated.
Abbreviations: RLA- Relative Luciferase Activity.

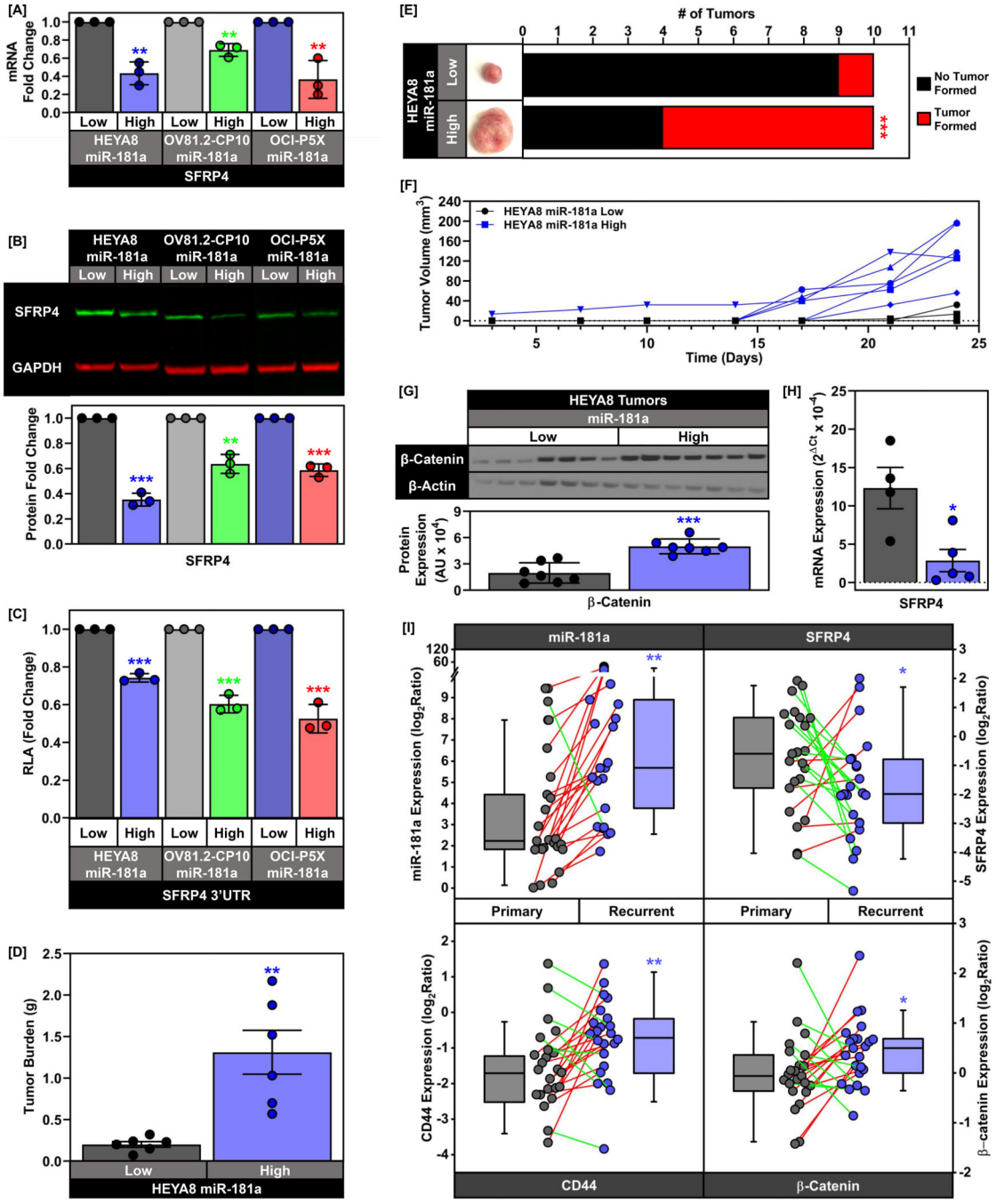

Figure 3: WNT/β-catenin inhibitor SFRP4 is a novel target of miR-181a

(A) Graph showing SFRP4 mRNA expression in the miR-181a^{Low} vs miR-181a^{High} EOC cells. (B) Western Blot showing SFRP4 protein expression in the miR-181a^{Low} vs miR-181a^{High} EOC cells with quantification below. (C) Graph showing SFRP4 3'UTR Reporter Activity for the miR-181a^{Low} vs miR-181a^{High} EOC cells. (D) Graph showing tumor burden for the in vivo limiting dilution tumor formation HEYA8 miR-181a^{Low} vs miR-181a^{High} mouse groups. (E) Representative images of miR-181a^{Low} vs miR-181a^{High} tumors (left) for the in vivo limiting dilution tumor formation assay with quantification of

the number of tumors formed in each group (right). (F) Graph of tumor kinetics for the HEYA8 miR-181a^{Low} vs miR-181a^{High} mouse groups. (G) Western blot showing β-catenin protein expression in the HEYA8 miR-181a^{Low} and HEYA8 miR-181a^{High} tumors with quantification below. (H) Graph showing SFRP4 mRNA expression in the HEYA8 miR-181a^{Low} and HEYA8 miR-181a^{High} tumors. (I) Box plot showing differences in miR-181a, SFRP4, CD44, and β-catenin expression in 22 matched primary vs recurrent patient high grade serous ovarian cancer tumors. Individual sets of matched primary and recurrent tumors are connected by solid lines. Green lines indicate a decrease in expression between primary vs recurrent and red lines indicate an increase between primary vs recurrent. All data are representative of 3 independent experiments. * = $p<0.05$, ** = $p<0.005$, *** = $p<0.0005$. Error bars indicate ±standard deviation unless otherwise stated. Abbreviations: RLA- Relative Luciferase Activity.

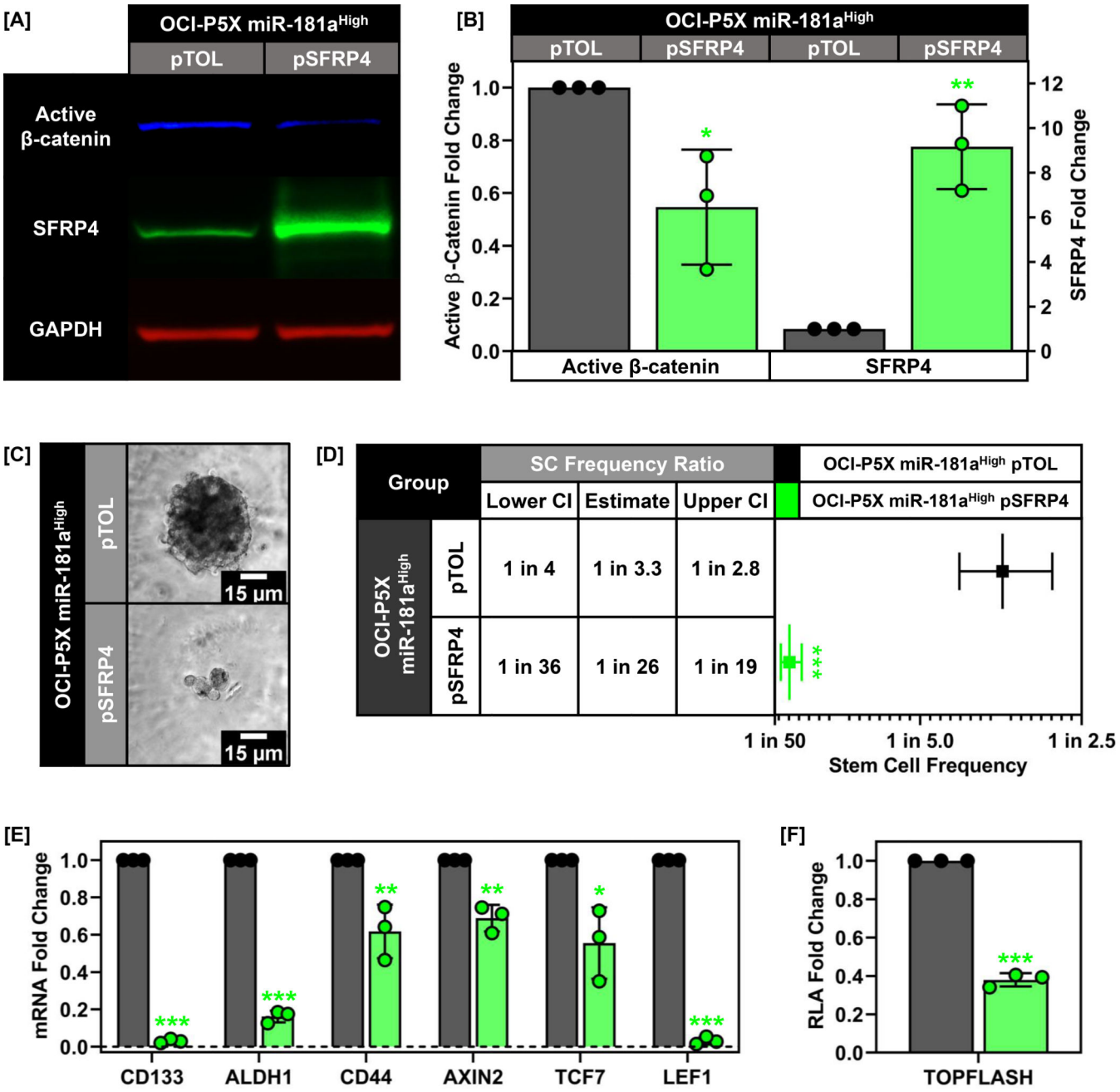

Figure 4: SFRP4 inhibits tumor initiating cell properties in miR-181a high EOC cells

(A) Western blot showing expression of active β-catenin and SFRP4 in OCI-P5X miR-181a^{High} pTOL vs pSFRP4 cells. (B) Quantification of active β-catenin and SFRP4 protein expression in OCI-P5X miR-181a^{High} and FT237 pmiR-181a pTOL vs pSFRP4 cells. (C) Micrographs showing representative ELDA tumor spheres for OCI-P5X miR-181a^{High} pTOL vs pSFRP4 cells. (D) Graph of log(Fraction Non-Responding) vs number of cells (left) and Stem Cell Frequency Ratio (right) for OCI-P5X miR-181a^{High} pTOL vs pSFRP4 cells. (E) Graph showing mRNA expression of stemness and WNT markers for OCI-P5X miR-181a^{High} and FT237 pmiR-181a pTOL vs pSFRP4 cells. (G)

Graph showing TOPFLASH luciferase activity for OCI-P5X miR-181a^{High} and FT237 pmiR-181a pTOL vs pSFRP4 cells. All data are representative of 3 independent experiments. * = $p<0.05$, ** = $p<0.005$, *** = $p<0.0005$. Error bars indicate ±standard deviation unless otherwise stated. Abbreviations: NR- Non-Responding, SC- Stem Cell, RLA- Relative Luciferase Activity.

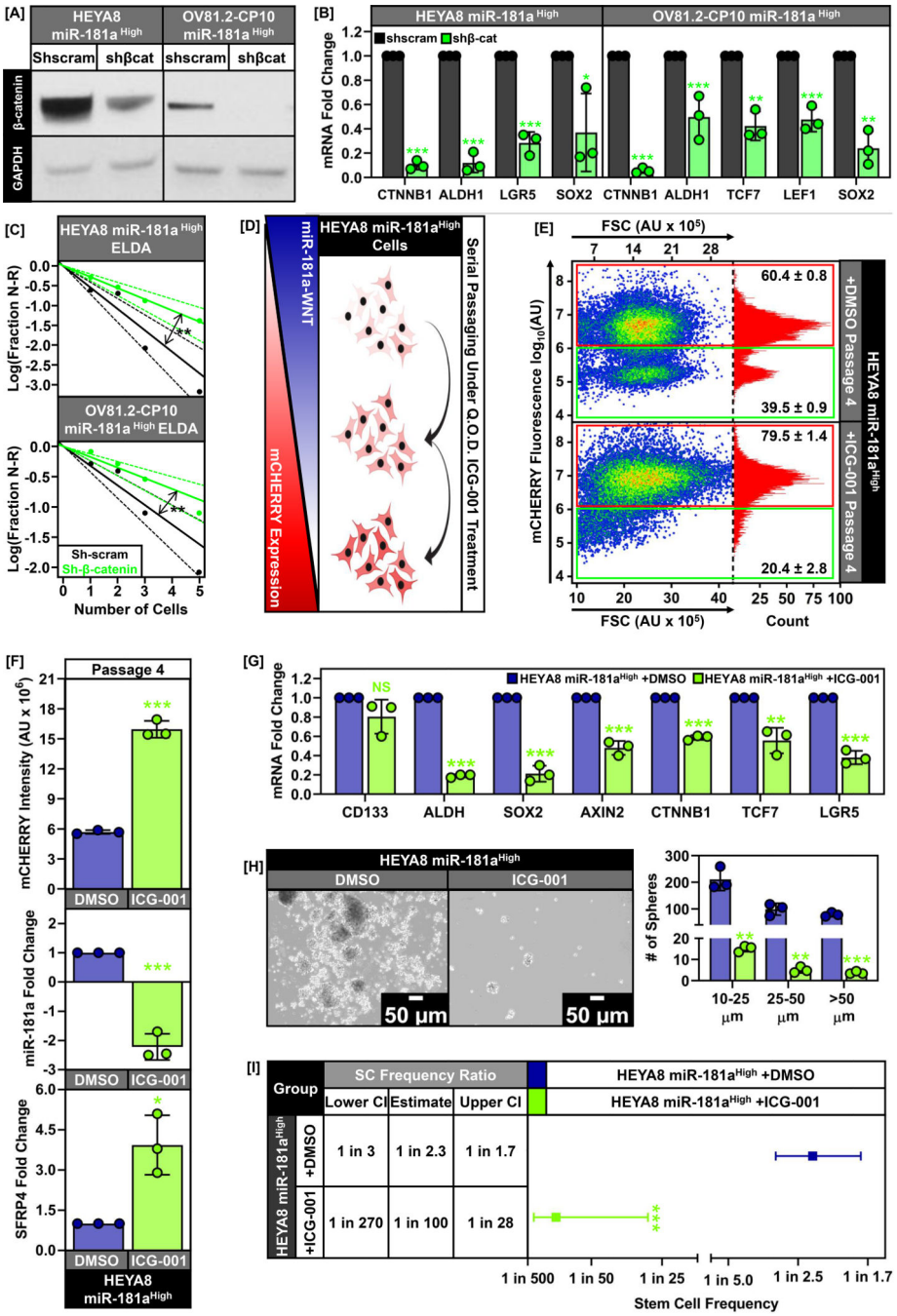

Figure 5: Inhibition of miR-181a activated WNT signaling decreases EOC tumor initiating cell properties

(A) Western blot showing β-catenin expression in HEYA8 and OV81.2 CP10 miR-181a^{High} shβcat vs shscram cells. (B) Graph showing decreased mRNA expression of stemness and WNT markers in HEYA8 and OV81.2 CP10 miR-181a^{High} shβcat vs shscram cells. (C) Graph showing decreased stem cell frequency in HEYA8 and OV81.2 CP10 miR-181a^{High} shβcat vs shscram cells. (D) Diagram showing strategy for targeting miR-181a/WNT high EOC cells using ICG-001. (E) Graphs showing mCHERRY fluorescence in HEYA8 miR-181a^{High} cells after 4 passages of Q.O.D. DMSO or 40 µM ICG-001 treatment. (F)

Graphs depicting mCHERRY intensity (top), miR-181a expression (middle), and SFRP4 expression (bottom) in HEYA8 miR-181a^{High} cells after 4 passages of Q.O.D. DMSO or 40 μM ICG-001 treatment. (G) Graph showing mRNA expression levels for HEYA8 miR-181a^{High} cells treated with either DMSO or 5 μM ICG-001 for 24 hours. (H) Representative micrographs showing tumor sphere formation for HEYA8 miR-181a^{High} cells treated with either DMSO or 5 μM ICG-001 for 24 hours. Quantification below. (I) Graph of log(Fraction Non-Responding) vs number of cells (left) and Stem Cell Frequency Ratio (right) for HEYA8 miR-181a^{High} treated with either DMSO or 5 μM ICG-001 for 24 hours. All data are representative of 3 independent experiments. * = $p<0.05$, ** = $p<0.005$, *** = $p<0.0005$. Error bars indicate ±standard deviation unless otherwise stated. Abbreviations: NR- Non-Responding, SC- Stem Cell.

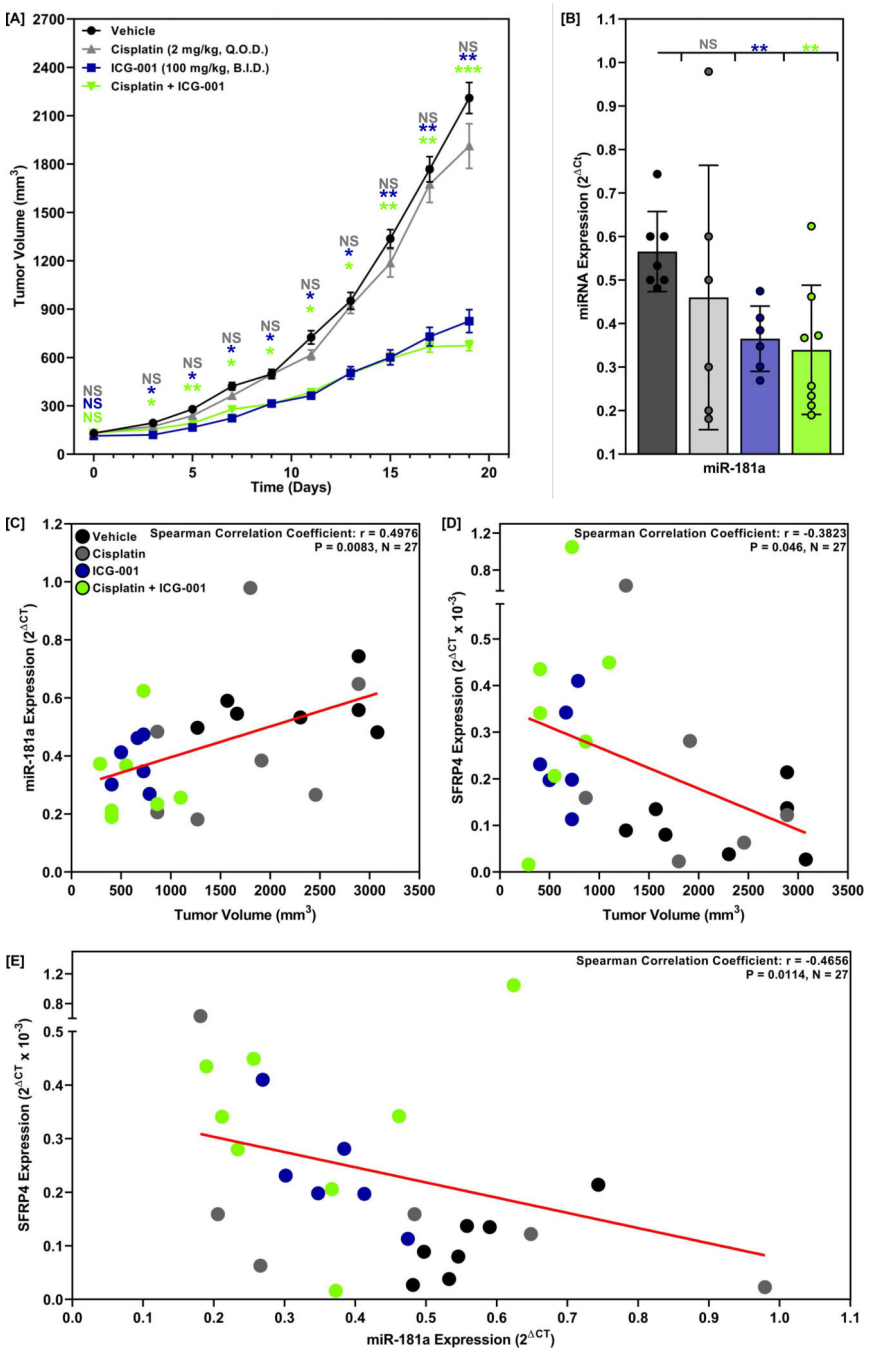

Figure 6: Therapeutic targeting of miR-181a-WNT signaling decreases EOC tumor growth in vivo

(A) Graph showing tumor kinetics for the PBS, Cisplatin, ICG-001, and Cisplatin + ICG-001 treatment groups. (B) Graph showing miR-181a expression across the PBS, Cisplatin, ICG-001, and Cisplatin + ICG-001 treatment groups. (C) Graph showing correlation between miR-181a (top) and SFRP4 (bottom) expression and final tumor volume for each treatment group. Data points are color coded according to treatment group. (D) Graph showing correlation between miR-181a and SFRP4 expression for each treatment group tumor. Data points are color coded according to treatment group. All data are

representative of 3 independent experiments. * = $p<0.05$, ** = $p<0.005$, *** = $p<0.0005$. Error bars indicate ±standard deviation unless otherwise stated.